Iron−Sulfur Cluster N7 of the NADH:Ubiquinone Oxidoreductase (Complex I) Is Essential for Stability but Not Involved in Electron Transfer[†]

Thomas Pohl, Theresa Bauer, Katerina Dörner, Stefan Stolpe, Philipp Sell, Georg Zocher, and Thorsten Friedrich*

Institut für Organische Chemie und Biochemie, Albert-Ludwigs-Universität Freiburg, Albertstrasse 21, Chemiehochhaus, D-79104 Freiburg i. Br., Germany

Received February 22, 2007; Revised Manuscript Received March 30, 2007

ABSTRACT: The NADH:ubiquinone oxidoreductase (complex I) from *Escherichia coli* is composed of 13 subunits called NuoA through NuoN. It catalyzes the electron transfer from NADH to ubiquinone by a chain of redox groups consisting of one FMN and seven iron−sulfur clusters. The function of the additional, nonconserved cluster N7 located on NuoG is not known. It has been speculated that it is not involved in electron transfer, due to its distance of more than 20 Å from the electron transfer chain. Dithionite-reduced minus NADH-reduced EPR difference spectra of complex I and of a soluble fragment containing NuoG revealed for the first time the EPR spectrum of N7 in the complex. Individual mutation of the cysteines ligating this cluster to alanine led to a decreased amount of complex I in the membrane without affecting the electron transfer activity. Sucrose gradient centrifugation revealed that the complex from the C230A and C233A mutants decayed in detergent solution while the C237A and C265A mutant complex was stable. Cluster N7 was detectable in the latter mutants but with shifted *g*-values, indicating a different ligation of N7. Thus, N7 is essential for the stability of the complex but is not involved in electron transfer.

The proton-translocating NADH:ubiquinone oxidoreductase (EC 1.6.99.3), also called respiratory complex I,[1] is the entry point for electrons into the respiratory chains of most eucaryotes and many bacteria (*1*−*6*). Its redox reaction is coupled with a translocation of protons across the membrane (*7*, *8*). One FMN and, depending on the species, up to nine iron−sulfur (Fe/S) clusters take part in electron transfer (*1*−*6*). In addition, two semiquinone radicals coined SQ_{Nf} and SQ_{Ns} have been identified as obligatory intermediates of the reaction (*6*, *9*, *10*).

The bacterial complex generally consists of 14 different subunits with seven hydrophilic proteins containing all known redox groups. The remaining seven subunits are very hydrophobic membrane intrinsic proteins. Electron microscopy revealed the two-part structure of the complex consisting of a peripheral arm with the hydrophilic proteins located in the aqueous milieu and a membrane arm with the hydrophobic proteins being buried in the lipid bilayer (*11*, *12*).

The structure of the peripheral arm of the *Thermus thermophilus* complex has been determined at 3.3 Å resolution revealing the localization of the redox groups and their participation in the electron transfer reaction (*13*). The primary electron acceptor FMN is located on NuoF (*13*). For sake of simplicity the *Escherichia coli* nomenclature for the subunits is used throughout. From the flavin one electron is most likely transferred to the tetranuclear Fe/S cluster N3 on the same subunit, while it is discussed that the second electron is probably temporarily "stored" on the binuclear cluster N1a (*13*−*15*). The electron on cluster N3 is transferred to the acceptor quinone via a chain made up of the binculear cluster N1b and the tetranuclear clusters N4 and N5 (all on NuoG), N6a and N6b on NuoI, and N2 on NuoB (*6*, *16*−*22*). After reoxidation of N3 by the electron transfer chain, the electron stored on N1a, which is located on NuoE 13 Å away from the FMN, could enter this chain via the FMN. It was proposed that this mechanism reduces the probability of producing superoxide radicals at the flavin in its semiquinone state (*13*).

In addition to these Fe/S clusters obviously involved in electron transfer, the tetranuclear Fe/S cluster N7 has been identified in the structure (*13*). The corresponding binding motif on subunit NuoG has so far been detected only in a few bacteria such as *E. coli*, *T. thermophilus*, *Aquifex aeolicus*, and *Salmonella thyphimurium* (*22*−*25*). This motif is made up of Cys^{230}, Cys^{233}, Cys^{237}, and Cys^{265} (*E. coli* numbering). The cluster coordinated by this motif has not yet been detected by EPR spectroscopy of the holoenzyme. It has been shown that a 10 kDa fragment of NuoG containing the motif is capable of binding a tetranuclear Fe/S cluster (*23*).

If cluster N7 does not participate in the physiological electron transfer reaction, it should not be reduced by NADH. Nevertheless, it could probably be chemically reduced by dithionite. Here we show that the EPR spectra of the preparations of the *E. coli* complex I and of the soluble NADH dehydrogenase fragment of complex I containing NuoG (*25*−*27*) exhibit signals from a tetranuclear Fe/S

[†] This work was supported by the Deutsche Forschungsgemeinschaft.

* Corresponding author. Phone: +49-(0)761-203-6060. Fax: +49-(0)761-203-6096. E-mail: tfriedri@uni-freiburg.de.

[1] Abbreviations: complex I, proton-pumping NADH:ubiquinone oxidoreductase; Dec-Q, decyl-ubiquinone, 2,3-dimethoxy-5-methyl-6-decylbenzoquinone; EPR, electron paramagnetic resonance; FMN, flavin mononucleotide; Fe/S, iron−sulfur; MES, 2-(*N*-morpholino)-ethanesulfonic acid; vis, visible.

10.1021/bi700371c CCC: $37.00
Published on Web 05/10/2007

cluster when the samples are reduced by dithionite. These signals are not present in the spectra of the preparations reduced by NADH and were thus attributed to N7. The four cysteine ligands of N7 were individually replaced with alanine. The mutants showed a decreased amount of complex I in the membranes but an unchanged specific activity. The complex was not stable in the C230A and C233A mutants. The complex from the C237A and C265A mutants showed the signals attributed to N7 in the EPR difference spectrum but with shifted *g*-values, indicating a different microenvironment of the cluster. We conclude that the EPR signals derive from cluster N7 and that it is essential for the assembly and the stability of complex I but that it does not participate in electron transfer.

EXPERIMENTAL PROCEDURES

Materials and Strains. *E. coli* strain ANN0221 is a *nuoB::nptI, ndh::tet* derivative of strain AN387 (*28*) and was generated using a genomic replacement method as described (*29*). In addition, *E. coli* strains DH5α (*30*), BL21(DE3) (*31*), and the plasmids pET11a/*nuoB-G*/NuoF$_C$ (*25*, *27*), pUM24 (*29*), pKD46, pKD4, pCP20 (*32*) and pBAD*nuo* containing the entire *nuo*-operon (T. Pohl, M. Uhlmann and T. Friedrich, unpublished data) were used in this study (for a detailed description, see Supporting Information, Tables S1 and S2). Ampicillin (100 μg/mL), chloramphenicol (170 μg/mL), and kanamycin (50 μg/mL) were supplemented where necessary. All enzymes used for recombinant DNA techniques were from Fermentas (St. Leon-Roth). DNA oligonucleotides were from Operon Biotechnologies (Cologne; Supporting Information, Table S3).

Recombineering. Transformants carrying pKD46 were grown aerobically in 100 mL of LB supplemented with ampicillin in a 300 mL of baffled conical flask at 30 °C. At an optical density at 600 nm (OD_{600}) of 0.25, L-arabinose was added to a final concentration of 0.2% (w/v) to induce the expression of the RED operon. The cells were grown to an OD_{600} of 0.4 and placed on ice for 10 min. First they were washed three times and then resuspended with ice-cold 10% (v/v) glycerol to an OD_{600} of 40. 50 μL of electrocompetent cells were mixed with DNA and electroporated at 17 kV/cm (Eppendorf electroporator 2510). The shocked cells were immediately mixed with 1 mL of SOC medium and incubated for 1 h at 37 °C. To select for recombinants, 200 μL of the cells was spread onto LB-agar supplemented with the appropriate antibiotic.

Chromosomal In-Frame Deletion of the nuo-Operon. The *nptI*-FRT cartridge was amplified from pKD4 by standard PCR using the primer pair *nuo::nptI* (Supporting Information, Table S3). Electrocompetent DH5α/pKD46 was mixed with 100 ng of PCR product and shocked as described above. Recombinants were selected on LB-agar supplemented with kanamycin. Km^R clones were selectively colony purified, and the site-specific integration of the *nptI*-FRT cartridge was checked by colony PCR with primer triples up, *nuo* down, *nptI* down and down, *nuo* up, *nptI* up (Supporting Information, Table S3) as described (*32*). Elimination of the *nptI*-FRT cartridge by FLP mediated recombination was performed as described (*32*).

Construction of Alanine Mutants. The *nptI-sacRB* cartridge was amplified from pUM24 by standard PCR with the primer pair *nuoG::nptI-sacRB* (Supporting Information, Table S3). Electrocompetent DH5αΔ*nuo*/pKD46 was mixed with 50 ng of pBAD*nuo* and 500 ng of PCR product. After recombineering, clones which had integrated the *nptI-sacRB* cartridge were selected on LB-agar supplemented with kanamycin. The plasmid DNA of Km^R mutants was isolated (*33*) and purified by transformation of DH5α and growth on LB-agar supplemented with kanamycin. The correct integration of the *nptI-sacRB* cartridge into pBAD*nuo* was verified by restriction analysis. To introduce the desired mutations on *nuoG*, the *nptI-sacRB* cartridge was replaced with a PCR product by recombineering (see Supporting Information, Figure S4). The *nuoG* fragments coding for the mutations C230A, C233A, C237A, and C265A (*25*) were amplified from pET11a/*nuoB-G*/NuoF$_C$ with the primer pair *nuoG* (Supporting Information, Table S3). Electrocompetent DH5α/pKD46 were co-transformed with 50 ng of pBAD*nuo nuoG::nptI-sacRB* and 300 ng of linear DNA as described above. Recombinants were selected on YP-agar supplemented with chloramphenicol and 10% (w/v) sucrose at 30 °C. The plasmids of Cam^R and Suc^S clones were isolated and analyzed by restriction analysis. The mutations were confirmed by DNA sequencing.

Growth of Cells and Isolation of the NADH Dehydrogenase Fragment. *E. coli* cells BL21(DE3) were transformed with pET11-a/*nuoB-G*/NuoF$_C$ (*25*). The resulting transformants were grown in 200 L culture of LB medium supplemented with 100 mg/L ampicillin, 100 mg/L ammonium sulfate, 10 mg/L ferric ammonium citrate, 50 mg/L riboflavin, and 0.5 mM L-cysteine. Cells were grown aerobically at 37 °C, and isopropyl β-D-thiogalactopyranoside was added (final concentration 0.4 mM) at an OD_{600} of 0.5. Three hours later the cells were harvested after entering the stationary growth phase. All steps during the preparation of the NADH dehydrogenase fragment were carried out at 4 °C. 30 g of cells (wet weight) was resuspended in 100 mL of 50 mM MES/NaOH, 60 mM NaCl, pH 6.0, 0.1 mM phenylmethanesulfonyl fluoride (PMSF), 10 μg/mL DNaseI, and 50 μg/mL lysozyme and disrupted by two passes through a French pressure cell (SLM Amicon) at 110 MPa. The cytoplasmic fraction was obtained by ultracentrifugation at 250000*g* for 60 min and applied to a 50 mL Fractogel EMD TMAE Hicap (Merck) column equilibrated in 50 mM MES/NaOH, 60 mM NaCl, pH 6.0 and 30 μM PMSF. Proteins were eluted with a 300 mL linear gradient from 60 mM to 300 mM NaCl in 50 mM MES/NaOH, pH 6.0. Fractions containing NADH/ferricyanide oxidoreductase activity were combined and applied to a 3 mL *Strep*-Tactin Sepharose column (IBA) equilibrated in 50 mM HEPES/NaOH, 60 mM NaCl, pH 7.5 and 30 μM PMSF. The NADH dehydrogenase fragment was eluted with 2.5 mM D-desthiobiotin in 60 mM NaCl, 50 mM MES/NaOH, pH 6.0. The fractions with NADH/ferricyanide oxidoreductase activity were pooled, concentrated by ultrafiltration (Centricon 100, Amicon), and stored at −80 °C.

Growth of Cells and Isolation of Complex I. *E. coli* cells ANN0221 were transformed with pBAD*nuo*. Parental and mutant *E. coli* strains were grown aerobically in 10 L culture of LB medium supplemented with 25 mM Na_2HPO_4, 25 mM KH_2PO_4, 50 mM NH_4Cl, 5 mM Na_2SO_4, 2 mM $MgSO_4$, and 0.1 mM ferric ammonium citrate at 37 °C. The expression of the *nuo*-operon was induced by addition of 0.2% L-

arabinose. The cells were harvested by continuous flow centrifugation at 16000*g*, 4 °C and stored at −80 °C until use. Wild type complex I of the control strain and the NuoG C265A variant were isolated similarly to the procedure described (*8*). All steps were carried out at 4 °C. Cells (40−50 g) were resuspended in a 5-fold volume of 50 mM MES/NaOH, 0.1 mM PMSF, pH 6.0, with 10 μg/mL DNAse I and 50 μg/mL lysozyme and disrupted by a single pass through a French pressure cell (SLM Aminco) at 110 MPa. Cell debris was removed by centrifugation at 36000*g* for 20 min, and cytoplasmic membranes were obtained by centrifugation at 250000*g* for 1 h. The membranes were resuspended in 50 mM MES/NaOH, 50 mM NaCl, pH 6.0 at a protein concentration of 80 mg/mL. *n*-Dodecyl-β-D-maltopyranoside (DDM, AppliChem) was added to a final concentration of 3%, and the solution was gently homogenized and centrifuged for 20 min at 250000*g*. The supernatant was applied to a 120 mL Fractogel EMD TMAE Hicap M (Merck) column equilibrated in 50 mM MES/NaOH, 50 mM NaCl, and 0.1% DDM, pH 6.0. Bound proteins were eluted with a 150 mL linear gradient of 150−350 mM NaCl in 50 mM MES/NaOH, 0.1% DDM, pH 6.0 at a flow rate of 15 mL/min. Fractions containing NADH/ferricyanide oxidoreductase activity were combined, diluted with an equal volume 50 mM MES/NaOH, pH 6.0, and loaded onto an 80 mL Source 15Q (GE Healthcare) column equilibrated in 50 mM MES/NaOH, 50 mM NaCl, and 0.1% DDM, pH 6.0. The column was eluted with a 500 mL linear gradient of 125−275 mM NaCl in 50 mM MES/NaOH, 0.1% DDM, pH 6.0 at a flow rate of 5 mL/min. Fractions containing NADH/ferricyanide oxidoreductase activity were pooled and concentrated with a 100 kDa MWCO Amicon Ultra-15 centrifugal filter (Millipore). The concentrated protein solution was subjected to size-exclusion chromatography on a 450 mL Sephacryl S-300 HR (GE Healthcare) column in 50 mM MES/NaOH, 50 mM NaCl, and 0.1% DDM, pH 6.0, at a flow rate of 20 mL/h. Peak fractions of NADH/ferricyanide oxidoreductase activity were combined and stored at −80 °C.

EPR Spectroscopy. EPR measurements were conducted with a Bruker EMX 1/6 spectrometer operating at X-band. The sample temperature was controlled with an Oxford instrument ESR-9 helium flow cryostat. The magnetic field was calibrated using a strong or a weak pitch standard. The isolated complex I (3 mg/mL) was reduced either with a few grains of dithionite or with a 1000-fold molar excess of NADH (*34*). The samples reduced by dithionite were diluted by the same volume of buffer as used for the reduction by NADH. The EPR spectra were simulated as described (*26*).

Enzyme Activity. Complex I activity in cytoplasmic membranes was measured either as NADH/ferricyanide oxidoreductase activity or as NADH oxidase activity (*35*, *36*). The NADH oxidase activity was inhibited by addition of 20 μM piericidin A, a specific complex I inhibitor (*35*). The NADH:decyl-ubiquinone oxidoreductase activity of isolated complex I was determined as described (*29*).

Other Analytical Procedures. Protein concentration was measured by the biuret method using BSA as standard. SDS−PAGE was performed according to Schägger and von Jagow (*37*) using a 10% T, 3% C separating gel. The concentration of the isolated proteins was determined by their absorbance at 280 nm using an extinction coefficient of 764 mM^{-1} cm^{-1} for complex I and 190 mM^{-1} cm^{-1} for the NADH dehydrogenase fragment as derived from the corresponding DNA sequences. Sucrose-gradient centrifugation in the presence of 0.1% DDM was performed as described (*34*).

RESULTS

Generation of Mutant Strains by λ-RED Mediated Recombineering. E. coli strain ANN0221 is devoid of any membrane-bound NADH dehydrogenase due to an inactivation of the gene coding for the alternative NADH dehydrogenase (*ndh*) by insertion of a tetracyclin resistance cartridge and inactivation of *nuoB* by insertion of a *nptI* resistance cartridge (*36*). Strain ANN0221 is coined parental strain. The plasmid pBAD*nuo* contains the entire *nuo*-operon under control of the arabinose-inducible P_{araBAD} promoter (T. Pohl, M. Uhlmann, and T. Friedrich, unpublished data). Transformation of ANN0221 with pBAD*nuo* resulted in strain ANN0221/pBAD*nuo*. This strain is coined control strain. The NADH-dependent catalytic activities of the cytoplasmic membranes of the control strain derive exclusively from the expression of the *nuo*-genes from the plasmid. Complex I from this strain is called the wild type complex. The mutations of the four cysteines comprising the binding motif for N7 to alanines were introduced on the plasmid pBAD*nuo*. A scheme illustrating the strategy used to generate the mutants by recombineering is presented in the Supporting Information (Figure S4). Transformation of ANN0221 with pBAD*nuo* containing the individual mutations led to the generation of the corresponding mutant strains. The NADH/ferricyanide reductase activity and the NADH oxidase activity of the cytoplasmic membranes of these mutant strains directly reflect the effect of the complex I mutations introduced.

Mutation of pBAD*nuo* by λ-RED mediated recombineering using *sacB* as a marker for counterselection led to an increased number of false positive clones that had lost the *nptI-sacRB* cartridge without acquiring the desired mutation. Since recombineering was performed in strain DH5α with a nuo^+ chromosomal background, the false positives clones were most likely generated by a recombination between the chromosomal and episomal-encoded *nuo*-operon in cells expressing the λ-RED functions. Therefore, strain DH5αΔ*nuo* was constructed as a host of manipulating pBAD*nuo*. The 15 kbp *nuo*-operon was replaced with a *nptI*-FRT cartridge (*32*) by recombineering using homology extensions of 49 and 50 nt, respectively. Several hundred Km^R clones were obtained by using 100 ng of PCR product. Colony PCR of five clones confirmed the correct integration of the resistance cartridge. FLP mediated recombination (*32*) resulted in strain DH5αΔ*nuo*. This strain was well suited for the manipulation of plasmid pBAD*nuo* by λ-RED mediated recombineering. After counterselection in the presence of 10% sucrose, around 50% of the Suc^R clones had the desired mutation in pBAD*nuo* as confirmed by restriction analysis and DNA sequencing.

EPR Spectrum of N7 in Complex I. The structure of the peripheral arm of the *T. thermophilus* complex I implied that N7 is not involved in the physiological electron transfer and therefore should not be reducible by NADH. However, if it is chemically reducible by dithionite, the EPR difference

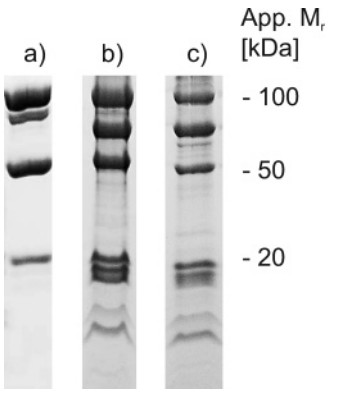

FIGURE 1: SDS−PAGE of the preparation of the NADH dehydrogenase fragment (a), wild type complex I (b), and complex I from the NuoG C265A mutant (c). The gel was stained with Coomassie brilliant blue. The band below NuoG in (a) corresponds to a proteolytically cleaved fragment of NuoG (*27*).

spectrum of a dithionite-reduced minus an NADH-reduced sample should display its spectrum. Complex I was prepared from the cytoplasmic membranes of the control strain by extraction of the membrane proteins with dodecyl maltoside and chromatography on Fractogel EMD, Source 15Q, and Sephacryl S-300 in the presence of dodecyl maltoside similarly to the procedure described (*8*). Fractions without any impurities as judged by SDS−PAGE were used for EPR spectroscopy (Figure 1). The sample was concentrated to 3 mg/mL, and two aliqouts were withdrawn. One aliquot was reduced by a 1000-fold molar excess NADH, the other with few grains of dithionite. The spectra of the samples reduced either by NADH or by dithionite obtained at 40 K and 2 mW microwave power showed the presence of the binuclear clusters N1a ($g_{x,y,z}$ = 1.92, 1.94, and 2.00) and N1b ($g_{\|,\perp}$ = 2.03 and 1.94; Figure 2). No difference was detectable concerning the *g*-values and the line width of the signals due to the reduction either by NADH or by dithionite. The amplitude of the signals of cluster N1b was approximately 15% greater in the sample reduced by NADH than in the sample reduced by dithionite. The signals of the tetranuclear Fe/S clusters N2 ($g_{\|,\perp}$ = 1.91 and 2.05), N3 ($g_{x,y,z}$ = 1.88, 1.92, and 2.04), and N4 ($g_{x,y,z}$ = 1.89, 1.93, and 2.09) were present in the spectrum recorded at 13 K and 5 mW microwave power in addition to the signals of the binuclear clusters (Figure 2). The signal amplitudes of cluster N3 and N4 were 5% to 10% greater in the sample reduced by dithionite. Due to an overlap with signals from an additional Fe/S cluster reduced by dithionite but not by NADH, it was not possible to determine a possible difference in the degree of reduction of N2. The signals of this additional Fe/S cluster were clearly present in the spectrum of the dithionite-reduced sample and not in the NADH-reduced sample (Figure 2).

These signals were visualized by subtracting the spectrum of the NADH-reduced sample from the spectrum of the dithionite-reduced sample (Figure 3). The spectrum exhibited rhombic symmetry with signals at $g_{x,y,z}$ = 1.895, 1.95, and 2.047 (Figure 3). The g_y-signal is slightly disturbed by signals resulting from the different degree of reduction of N1b, N3, and N4 in the two samples which all contribute to 1.95 *g*-region (*6, 34*). As the additional signals were visible at temperatures below 20 K (Figure 2), they most likely derive from a tetranuclear Fe/S cluster. Spin quantification of the signals showed that they were present in

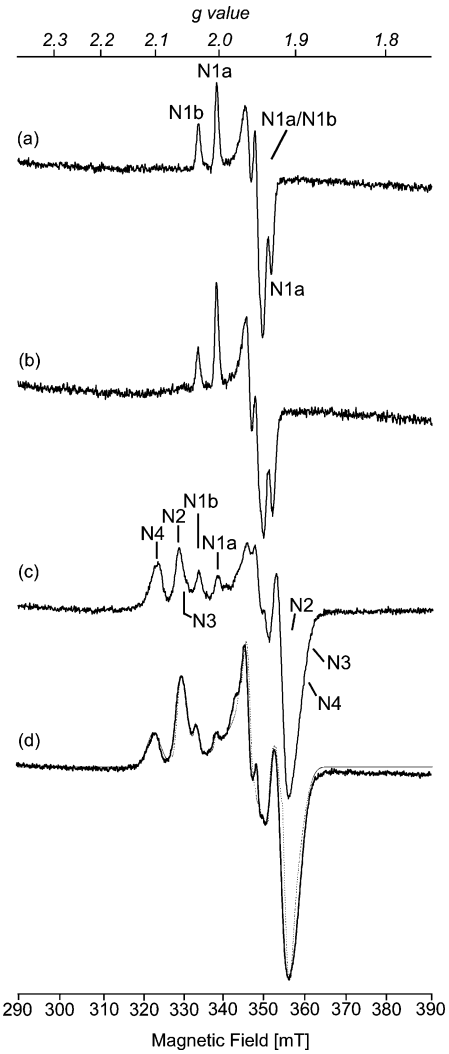

FIGURE 2: EPR spectra of the wild type complex I isolated from the control strain. Aliquots were reduced either by NADH (a, c) or by dithionite (b, d). The spectra were recorded either at 40 K and 2 mW (a, b) or at 13 K and 5 mW (c, d). The gray spectrum in (d) shows a simulation of the spectrum using the following spin contributions of individual clusters: N1a/N1b/N2/N3/N4/N7 = 0.45:0.1:1.00:0.82:1.25:0.78. The position of the signals of the individual clusters is indicated. The binuclear clusters N1a and N1b are highly saturated under these conditions. Other EPR conditions: microwave frequency, 9.44 GHz; modulation amplitude, 0.6 mT; time constant, 0.164 s; scan rate, 17.9 mT/min.

stoichiometric amounts relative to the other clusters in the preparation, making it very unlikely that these signals derived from an impurity or resulted from cluster deterioration (Figure 2). As the signals were only seen in the dithionite-reduced sample of complex I, they were tentatively attributed to cluster N7. The spectrum of N7 in complex I was simulated with the following parameters: $g_{x,y,z}$ = 1.894, 1.953, and 2.047 and linewidths of $L_{x,y,z}$ = 2.8, 1.75, and 2.2 mT (Figure 3).

EPR-Spectra of N7 in the NADH Dehydrogenase Fragment. To check whether the additional signals detected in complex I by EPR difference spectroscopy derived from an impurity of the preparation, we performed the same experiment with the NADH dehydrogenase fragment of the complex. The NADH dehydrogenase fragment is made up of the subunits NuoE, F, and G and should therefore also contain cluster N7 (*26*, *27*). The NADH dehydrogenase

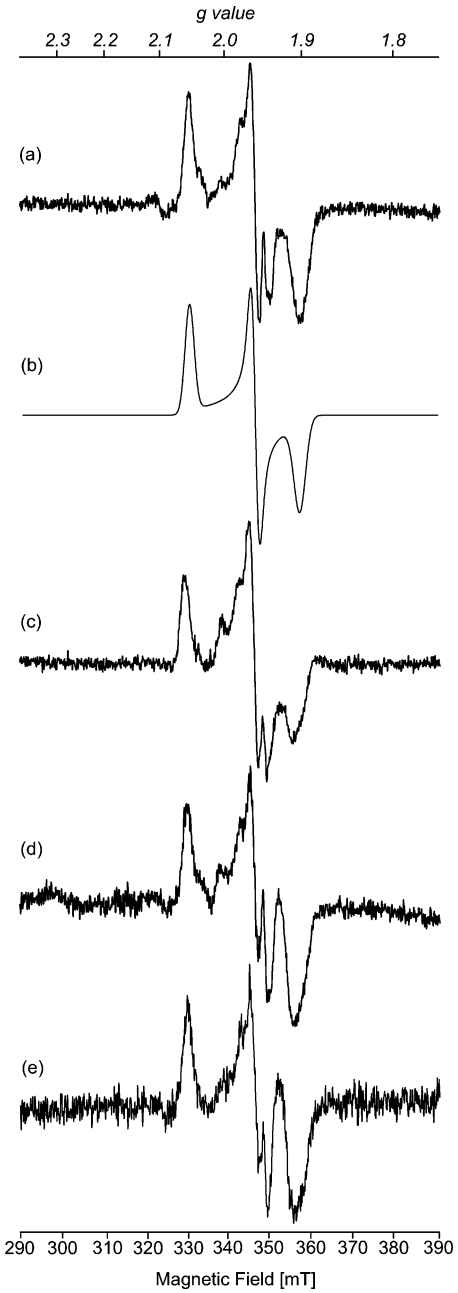

FIGURE 3: Dithionite-reduced minus NADH-reduced EPR difference spectra at 13 K and 5 mW. The difference spectra of wild type complex I (a), the NADH dehydrogenase fragment (c), the NuoG C265A complex I variant (d), and the NuoG C237A variant (e) are shown. Spectrum (b) shows the simulation of spectrum (a) using the parameters described in the text.

fragment was isolated from the cytoplasmic fraction of an overproducing strain with slight modifications of the procedure described (*25*, *27*) by anion exchange chromatography on Fractogel EMD and affinity chromatography on *Strep*-Tactin (Figure 1). The preparation was concentrated to 3 mg/mL, and one aliquot was reduced by NADH and another one by dithionite as described above. The EPR spectra at 40 K revealed the presence of the two binuclear clusters (data not shown). With this preparation the signal amplitudes from N1a were independent from the type of reductant while those from N1b were 15% greater on reduction by dithionite. At 13 K the signals of clusters N3 and N4 were detected. Cluster N2 is not present in this fragment due to the lack of subunit NuoB (*20*, *26*). Subtraction of the spectrum of the NADH-reduced sample from that of the dithionite-reduced sample revealed the presence of additional signals (Figure 3). As with complex I, the additional signals were detectable in the NADH dehydrogenase fragment at low temperatures. The spectrum showed rhombic symmetry with *g*-values very similar to those obtained with the complex I preparation ($g_{x,y,z}$ = 1.90, 1.95, and 2.053). Spin quantitation revealed that the signal was present in stoichiometric amounts compared to the other clusters detected in the preparation (N3/N4/N7 = 1.0:0.88:0.85). Thus, a tetranuclear Fe/S cluster with nearly identical spectral properties and which was only reducible with dithionite but not with NADH is present in complex I and in the NADH dehydrogenase fragment of the complex. As both preparations contain subunits NuoE, F, and G and all other Fe/S clusters including cluster N5 harbored by these subunits have been shown to be reducible with NADH (*6*, *26*, *34*, *38*), it is reasonable to assume that the signals obtained by difference spectroscopy derive from the Fe/S cluster N7. It is very unlikely that the signals were due to an impurity in the preparations because the samples were obtained by different purification procedures.

Catalytic Activity of the Mutants. Mutations were generated on pBAD*nuo* replacing the four cysteines on NuoG comprising the binding motif for N7 individually by alanine using λ-RED-mediated recombineering. The enzymatic activities of the mutants were determined at least with two independent cultures. The amount of complex I in the membranes was estimated from the respective NADH/ferricyanide oxidoreductase activity (Table 1). The parental strain ANN0221 did not show any enzymatic activity indicating the loss of both membrane-bound NADH dehydrogenases. The control strain ANN0221/pBAD*nuo* showed a 4-fold increased NADH/ferricyanide oxidoreductase activity compared to the B-wild type strain and an activity similiar to strain ANN003/pAR1213 overproducing complex I due to the replacement of the *nuo*-operon promoter on the chromosome (*29*). Compared to the control strain the complex I content was approximately halved in the C230A, C233A, and C237A mutant strains and reduced by one-fifth in the C265A mutant strain (Table 1).

The physiological activity of complex I was measured as NADH oxidase activity (Table 1). This activity was not detectable in the parental strain, and the control strain showed an NADH oxidase activity similar to strain ANN003/pAR1213 (*29*). The activity of the complex in the NuoG mutants was deduced from the NADH oxidase activity normalized to the amount of the complex in the membranes as calculated from the NADH/ferricyanide oxidoreductase activity. Compared to the control strain, the rate was reduced by less than 20% in the mutants C233A, C237A, and C265A. It was reduced by 30% in the mutant C230A. This activity was fully sensitive to piericidin A, a specific complex I inhibitor. These data indicated that a fully assembled complex I was active with insignificantly reduced rates in the mutant membranes.

Stability of Complex I from the Mutants. The reduced amount of complex I as determined by the reduced NADH/ferricyanide oxidoreductase activity of the mutant strains (Table 1) could be due to a reduced stability of the complex in the mutants. To examine this possibility, the membrane proteins were extracted from the mutants and from the control strain by dodecyl maltoside and separated on a sucrose

Table 1: Enzyme Activities of Complex I in the Membrane Fraction of Various *E. coli* Strains Used in This Study[a]

strain	NADH/ferricyanide oxidoreductase activity [μmol min^{-1} mg^{-1}]	NADH oxidase activity [μmol min^{-1} mg^{-1}]	inhibition by piericidin [%]	normalized NADH oxidase activity [μmol min^{-1} mg^{-1}]
ANN0221	0.09	0	–	–
ANN0221/pBAD*nuo*	2.89	0.52	94	0.52
ANN0221/pBAD*nuo nuoG* C230A	1.62	0.20	85	0.36
ANN0221/pBAD*nuo nuoG* C233A	1.01	0.17	90	0.49
ANN0221/pBAD*nuo nuoG* C237A	1.55	0.23	95	0.43
ANN0221/pBAD*nuo nuoG* C265A	2.30	0.33	95	0.42

[a] The NADH oxidase activity of the mutant strains was normalized by the ratios of the NADH/ferricyanide oxidoreductase activity of wild type and mutant strains.

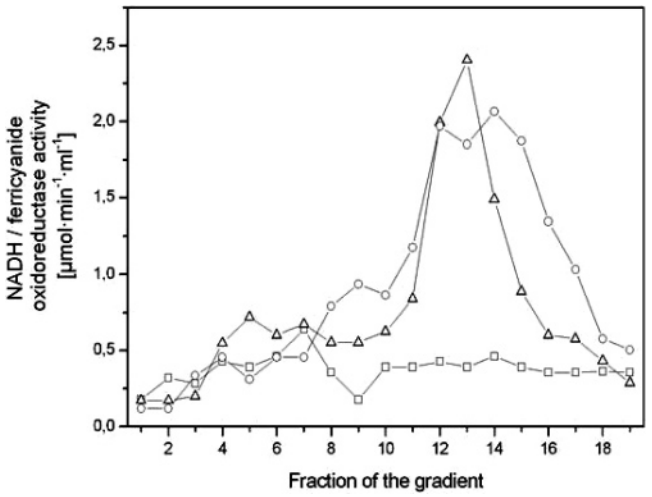

FIGURE 4: Sucrose gradient centrifugation of detergent extracts of cytoplasmic membranes of strains ANN0221/pBADnuo (○), ANN0221/pBADnuo/nuoG C233A (□), and ANN0221/pBADnuo/nuoG C265A (△). Proteins were extracted from cytoplasmic membranes with 3% dodecyl maltoside (w/v) and separated in gradients from 5% to 30% sucrose in 50 mM MES/NaOH, 50 mM NaCl, 5 mM $MgCl_2$ and 0.1% dodecyl maltoside, pH 6.0. The gradients were loaded with 17−20 mg of protein, and the activities shown were calculated to the same amount of 10 mg of protein to allow a direct comparison. Fractions of the gradients (numbered 1−19 from top to bottom) were collected and analyzed for NADH/ferricyanide oxidoreductase activity. The extracts from the C230A mutant showed a sedimentation profile similar to the C233A mutant and extract from the C237A mutant a profile like that of the C265A mutant.

gradient as described (*34*). The gradient was fractioned, and the NADH/ferricyanide oxidoreductase activity of the fractions was determined (Figure 4). The presence of a fully assembled and stable complex I is indicated by an activity peak at two-thirds of the gradient (*34*). Sucrose gradient centrifugation showed the presence of a stable complex I in the cytoplasmic membranes of the control strain and the C237A and C265A mutants (Figure 4). The C265A mutant contained a larger amount of stable complex I than the C237A mutant. In contrast, the NADH/ferricyanide oxidoreductase activity peak was not detectable in the membranes of the C230A and C233A mutants (Figure 4). Thus, the latter mutations restricted the stability of the complex such that it decayed in detergent solution while the former did not influence its stability.

Isolation of Complex I from the C265A Mutant. To determine whether complex I assembled in the C265A mutant contained cluster N7, we isolated the enzyme from the mutant and characterized the preparation by its enzymatic and EPR-spectroscopic properties. The complex from the C265A mutant eluted from the anion-exchange chromatography on Source 15Q at 250 mM NaCl and after 220 mL from the Sephacryl S-300 size-exclusion column (Supporting Information, Figure S6). On average, 3 mg of complex I was obtained from 80 g of cells (Supporting Information, Table S5). Wild type complex I was prepared from the control strain by the same method. Both preparations were reconstituted in phospholipids as described (*8*), and the kinetic parameters with NADH and decyl-ubiquinone as substrates were determined. It turned out that the wild type complex and the C265A variant exhibited virtually the same catalytic properties in the range of the limits of the method. The $K_M^{(NADH)}$ and $K_M^{(Dec-Q)}$ were determined to be 10 and 3 μM, respectively, for both preparations. The v_{max} was determined to be 2.9 μmol of NADH/(min mg) for the wild type complex and to be 2.0 μmol of NADH/(min mg) for the C265A variant. The reaction of both preparations was completely sensitive to piericidin A. In contrast, the preparation of the complex from the C237A mutant was not stable and decayed rapidly.

EPR-Spectroscopic Characterization of Complex I from the C265A Mutant. The preparation of the C265A variant was concentrated to 2 mg/mL. One aliquot was reduced by a 1000-fold molar excess NADH and another with a few grains of dithionite. The EPR spectrum recorded at 40 K revealed the presence of the binuclear clusters N1a and N1b in stoichiometric amounts with the same spectral characteristics as in the wild type (data not shown). The EPR spectrum of the C265A variant reduced by dithionite contained additional signals compared to the spectrum obtained from the sample reduced by NADH. The dithionite-reduced minus NADH-reduced EPR difference spectrum clearly revealed the signals attributed to N7 (Figure 3). The signals showed a rhombic symmetry with $g_{x,y,z} = 1.901$, 1.95, and 2.049 (Figure 3). The shape of the signal and the position of the *g*-values were similar but not identical to those obtained from the wild type complex (Figure 3). As the signals stem from the same Fe/S cluster, the shift in the *g*-values resulted from a change in its microenvironment. Thus, the mutation C265A led to a different ligation of the cluster corroborating that the signals shown in Figure 3 stem from the Fe/S cluster N7. The amount of N7 in the variant relative to the other clusters was the same compared to the wild type complex indicating that a stable preparation of the *E. coli* complex I can only be obtained with a complex containing N7. It is reasonable to assume that the presence of N7 in complex I from this mutant stabilizes the complex enabling its preparation. Cluster N7 was also detectable in a preparation of the complex from the mutant C237A, again, with shifted

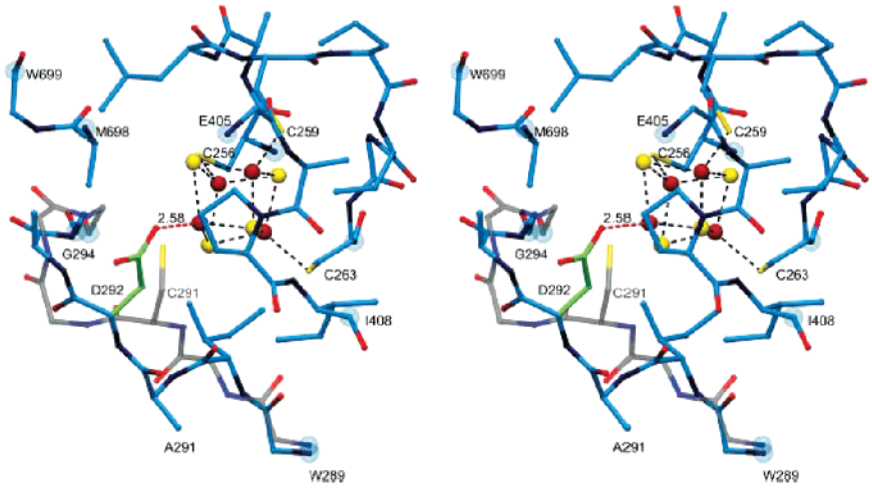

FIGURE 5: Stereoview of the environment of the N7 binding site. The coordinates were taken from the structure of the peripheral arm of *T. thermophilus* complex (PDB entry 2FUG). The loop of chain 3 (corresponding to NuoG) consisting of the amino acids W289 to G294 from 2FUG was retraced using RAPPER (*46*) and COOT (*47*). All modeled residues were built with respect to reasonable Ramachandran angles. The figure was generated using POVscript+ and POVRAY (www.povray.org).

g-values compared to the spectrum of the wild type complex (Figure 3).

A possible explanation for the presence of cluster N7 in the C265A mutant complex and the resulting stability of the preparation is the presence of an alternative cluster ligand. According to the structure of the peripheral arm of the complex (*13*), a candidate for this ligand is D266 in *T. thermophilus* complex I. It has been proposed that an aspartic acid residue is capable of ligating an Fe/S cluster either directly or by a bridging water molecule (*39*, *40*). The *T. thermophilus* D266 on NuoG corresponds to D292 of the *E. coli* sequence. D292 could be a direct ligand of N7. This coordination would lead to a twist of the polypeptide backbone from W289 to G294 (Figure 5). The dihedral angles resulting from the change of the backbone position are in the allowed region of a Ramachandran plot.

DISCUSSION

The *E. coli* complex I subunits contain nine motifs for the binding of Fe/S clusters (*41*). So far, the clusters N1a, N1b, N2, N3, and N4 have been detected by EPR-spectroscopy (*24*, *25*, *29*, *34*, *42*) and the clusters N6a and N6b by UV/vis-spectroscopy (*19*). The fast relaxing tetranuclear cluster N5 located on NuoG has been detected in the complex from other species (*38*, *43*) and in the overproduced single NuoG subunit of the *E. coli* complex I (*24*), but not in the holo-enzyme. It has been shown that N5 is reduced by NADH (*38*). An EPR spectrum of N7 on NuoG in complex I has so far not been reported.

In early studies, it was mistakenly assumed that the additional binding motif on NuoG was used to ligate a binuclear Fe/S cluster coined N1c, which had been detected by EPR-spectroscopy (*34*, *42*). Later site-directed mutagenesis studies showed that the EPR signals attributed to N1c derived from N1a and that there is no cluster N1c in complex I (*25*). An EPR spectrum of the cluster ligated by the additional Fe/S cluster binding motif on NuoG was obtained from a short fragment of the homologous subunit of the *T. thermophilus* complex I and the overproduced *E. coli* NuoG subunit (*23*, *24*). The Fe/S cluster bound to the additional binding motif on NuoG has been coined N7 (*23*−*25*).

From the EPR-spectroscopic analysis of the *T. thermophilus* NuoG fragment and the *E. coli* NuoG single subunit reconstituted with iron and sulfide it was proposed that a tetranuclear cluster is bound by this motif. This proposal was confirmed by the structure of the peripheral arm of complex I at molecular resolution (*13*). The EPR spectrum of the cluster exhibited rhombic symmetry with $g_{x,y,z} = 1.91$, 1.94, and 2.05 and $L_{x,y,z} = 2.1$, 1.2, and 1.25 mT (*24*). The EPR spectral properties of cluster N7 in complex I described here are very similar but not identical to those found with overproduced NuoG subunit. The spectrum was detectable only at temperatures below 20 K and showed a rhombic symmetry with $g_{x,y,z} = 1.894$, 1.953, and 2.047 and $L_{x,y,z} =$ 2.8, 1.75, and 2.2 mT (Figure 3). These signals derive from cluster N7 because they were detected with complex I and with the NADH dehydrogenase fragment of the complex, which were obtained from cytoplasmic membranes and the cytoplasmic fraction, respectively, by different purification protocols. In addition, they were present in stoichiometric amounts compared to the other clusters of the complex. Thus, it is most unlikely that these signals derive from an impurity. Furthermore, the *g*-values were slighty shifted in the NuoG C237A and C265A variants (Figure 3), indicating that the mutation changed the environment of the cluster.

Cluster N7 was reduced by dithionite but not by NADH (Figure 2), demonstrating that it is not involved in the physiological electron transfer reaction. This has been proposed based on the structure of the peripheral arm. The distance of N7 to the electron transfer chain is too long to allow its participation (*13*). It could be argued that the midpoint potential of N7 is very low and therefore N7 is not reduced by NADH. In a first crude attempt to determine the midpoint potential of N7 we obtained an $E_{m,6}$ of -250 ± 40 mV (T. Pohl and T. Friedrich, unpublished results). Thus, the midpoint potential of N7 is not the cause that N7 is not reduced by NADH. Due to the spectral overlap with N2 a more detailled study to determine the precise midpoint potential has to be performed. Taking all together, it is very unlikely that N7 is involved in the reduction of menaquinone under anaerobic conditions as it has been proposed (*44*). However, it cannot be completely ruled out that menaquinone

binding induces conformational changes that shorten the distance of N7 either to the electron transfer chain or to a putative menaquinone binding site although no experimental evidence corroborating this assumption has been presented.

Our data show that the cluster is important for the assembly and the stability of the complex (Table 1, Figure 4). Mutagenesis of the cysteine residues coordinating N7 led to a reduced content of complex I in the mutant membranes (Table 1). Thus, the assembly of the complex was slightly disturbed by the mutations introduced. The C230A and C233A mutations led to a strongly decreased stability of the complex as indicated by the complete loss of complex I activity upon sucrose gradient centrifugation in dodecyl maltoside (Figure 4). The effect of the mutations C237A and C265A was not so pronounced because the complex contained cluster N7 in these mutants (Figure 3). The amount of N7 relative to the other clusters of the complex was not significantly changed in the mutant complex, indicating that the preparations were exclusively made up of a protein population containing N7. It was not possible to isolate complex I from any mutant lacking N7. Thus, the presence of N7 is essential for the stability of complex I. These data are in accordance with the finding that the *in-trans* complementation of an *E. coli* chromosomal *nuoG* deletion led to a disturbed assembly of the complex when the binding motif for N7 is missing on the expression-plasmid containing *nuoG* (*24*). Mutagenesis of the N7 binding motif on NuoG in the NADH dehydrogenase fragment of the complex led to a reduced stability of the fragment (*25*). However, the effect of the individual mutations were different from those obtained here with the entire complex. The fragment was not detectable in the cytoplasmic fraction of the C230A and C265A mutant strains, but in the C233A and C237A mutants (*25*). A fully assembled NADH dehydrogenase fragment was isolated from the strains C233A, C237A, and C265A. However, the preparation of the fragment from the C237A mutant was very unstable. The different stability of the individual variants of the NADH dehdrogenase fragment and of complex I derive most likely from the interaction with the residual subunits conferring an additional stability to the complex I variants.

The fact that N7 was detectable in the preparations of the C237A and C265A variants is most likely due to a change in its ligation pattern. For the most stable C265A variant aspartic acid 292 could possibly replace cysteine 265 as cluster ligand (Figure 5). The change in the coordination of the cluster would induce a rearrangement of the NuoG backbone which would be sterically allowed and which would explain the shift of the *g*-values of the N7 EPR signals in this variant (Figure 3). The alternative ligand of the N7 in the C237A variant is not clear. The strongly reduced stability of this preparation could also be due to a missing fourth protein ligand of the cluster and a subsequent decay of the [4Fe-4S] cluster leading to a decay of the complex. However, EPR signals of a [3Fe-4S] cluster were not detected in an oxidized sample of the preparation of the C237A variant (data not shown). Thus, it is more likely that N260 replaces the cysteine ligand. A rotamer of N260 brings the carbonyl oxygen atom in 5 Å distance to the Fe atom. The coordination could be achieved by a non-protein ligand such as OH^- located between the carbonyl oxygen atom of N260 and the Fe atom as it has been described for a [2Fe-2S] cluster (*45*).

ACKNOWLEDGMENT

We thank Prof. Dr. G. Fuchs, Universität Freiburg, for the fermentation of *E. coli* BL21(DE3)/pET11-a/nuoB-G/NuoFc in a 200 l fermenter jar. We are grateful to Linda Böhm for her help in preparing the manuscript.

SUPPORTING INFORMATION AVAILABLE

Description of strains (Table S1) and plasmids (Table S2), oligonucleotides used for site-directed mutagenesis (Table S3), and scheme illustrating the strategy used to generate the mutants by recombineering (Figure S4). Isolation of *E. coli* complex I from strain ANN0221/pBAD*nuo*/*nuoG* C265A (Table S5), and isolation of *E. coli* complex I from strain ANN0221/pBAD*nuo*/*nuoG* C265A (Figure S6). This material is available free of charge via the Internet at http://pubs.acs.org.

REFERENCES

1. Walker, J. E. (1992) The NADH:ubiquinone oxidoreductase (complex I) of respiratory chains, *Q. Rev. Biophys. 25*, 253−324.
2. Friedrich, T., Steinmuller, K., and Weiss, H. (1995) The proton-pumping respiratory complex I of bacteria and mitochondria and its homologue in chloroplasts, *FEBS Lett. 367*, 107−111.
3. Friedrich, T. (2001) Complex I: a chimaera of a redox and conformation-driven proton pump?, *J. Bioenerg. Biomembr. 33*, 169−177.
4. Brandt, U., Kerscher, S., Drose, S., Zwicker, K., and Zickermann, V. (2003) Proton pumping by NADH:ubiquinone oxidoreductase. A redox driven conformational change mechanism?, *FEBS Lett. 545*, 9−17.
5. Yagi, T., and Matsuno-Yagi, A. (2003) The proton-translocating NADH-quinone oxidoreductase in the respiratory chain: the secret unlocked, *Biochemistry 42*, 2266−2274.
6. Ohnishi, T. (1998) Iron-sulfur clusters/semiquinones in complex I, *Biochim. Biophys. Acta 1364*, 186−206.
7. Bertsova, Y. V., and Bogachev, A. V. (2004) The origin of the sodium-dependent NADH oxidation by the respiratory chain of *Klebsiella pneumoniae*, *FEBS Lett. 563*, 207−212.
8. Stolpe, S., and Friedrich, T. (2004) The *Escherichia coli* NADH: ubiquinone oxidoreductase (complex I) is a primary proton pump but may be capable of secondary sodium antiport, *J. Biol. Chem. 279*, 18377−18383.
9. Ohnishi, T., Johnson, J. E., Jr., Yano, T., Lobrutto, R., and Widger, W. R. (2005) Thermodynamic and EPR studies of slowly relaxing ubisemiquinone species in the isolated bovine heart complex I, *FEBS Lett. 579*, 500−506.
10. Ohnishi, T., and Salerno, J. C. (2005) Conformation-driven and semiquinone-gated proton-pump mechanism in the NADH-ubiquinone oxidoreductase (complex I), *FEBS Lett. 579*, 4555−4561.
11. Grigorieff, N. (1999) Structure of the respiratory NADH:ubiquinone oxidoreductase (complex I), *Curr. Opin. Struct. Biol. 9*, 476−483.
12. Friedrich, T., and Böttcher, B. (2004) The gross structure of the respiratory complex I: a Lego System, *Biochim. Biophys. Acta 1608*, 1−9.
13. Sazanov, L. A., and Hinchliffe, P. (2006) Structure of the hydrophilic domain of respiratory complex I from *Thermus thermophilus*, *Science 311*, 1430−1436.
14. Sled, V. D., Rudnitzky, N. I., Hatefi, Y., and Ohnishi, T. (1994) Thermodynamic analysis of flavin in mitochondrial NADH: ubiquinone oxidoreductase (complex I), *Biochemistry 33*, 10069−10075.
15. Fecke, W., Sled, V. D., Ohnishi, T., and Weiss, H. (1994) Disruption of the gene encoding the NADH-binding subunit of NADH: ubiquinone oxidoreductase in *Neurospora crassa*. Formation of a partially assembled enzyme without FMN and the iron-sulphur cluster N-3, *Eur. J. Biochem. 220*, 551−558.
16. Moser, C. C., Farid, T. A., Chobot, S. E., and Dutton, P. L. (2006) Electron tunneling chains of mitochondria, *Biochim. Biophys. Acta 1757*, 1096−1109.

17. Flemming, D., Stolpe, S., Schneider, D., Hellwig, P., and Friedrich, T. (2005) A possible role for iron-sulfur cluster N2 in proton translocation by the NADH: ubiquinone oxidoreductase (complex I), *J. Mol. Microbiol. Biotechnol. 10*, 208−222.
18. Zu, Y., Di Bernardo, S., Yagi, T., and Hirst, J. (2002) Redox properties of the [2Fe-2S] center in the 24 kDa (NQO2) subunit of NADH:ubiquinone oxidoreductase (complex I), *Biochemistry 41*, 10056−10069.
19. Rasmussen, T., Scheide, D., Brors, B., Kintscher, L., Weiss, H., and Friedrich, T. (2001) Identification of two tetranuclear FeS clusters on the ferredoxin-type subunit of NADH:ubiquinone oxidoreductase (complex I), *Biochemistry 40*, 6124−6131.
20. Gurrath, M., and Friedrich, T. (2004) Adjacent cysteines are capable of ligating the same tetranuclear iron-sulfur cluster, *Proteins 56*, 556−563.
21. Zwicker, K., Galkin, A., Drose, S., Grgic, L., Kerscher, S., and Brandt, U. (2006) The Redox-Bohr group associated with iron-sulfur cluster N2 of complex I, *J. Biol. Chem. 281*, 23013−23017.
22. Friedrich, T. (1998) The NADH:ubiquinone oxidoreductase (complex I) from *Escherichia coli*, *Biochim. Biophys. Acta 1364*, 134−146.
23. Nakamaru-Ogiso, E., Yano, T., Ohnishi, T., and Yagi, T. (2002) Characterization of the iron-sulfur cluster coordinated by a cysteine cluster motif (CXXCXXXCX27C) in the Nqo3 subunit in the proton-translocating NADH-quinone oxidoreductase (NDH-1) of *Thermus thermophilus* HB-8, *J. Biol. Chem. 277*, 1680−1688.
24. Nakamaru-Ogiso, E., Yano, T., Yagi, T., and Ohnishi, T. (2005) Characterization of the iron-sulfur cluster N7 (N1c) in the subunit NuoG of the proton-translocating NADH-quinone oxidoreductase from *Escherichia coli*, *J. Biol. Chem. 280*, 301−307.
25. Uhlmann, M., and Friedrich, T. (2005) EPR signals assigned to Fe/S cluster N1c of the *Escherichia coli* NADH:ubiquinone oxidoreductase (complex I) derive from cluster N1a, *Biochemistry 44*, 1653−1658.
26. Braun, M., Bungert, S., and Friedrich, T. (1998) Characterization of the overproduced NADH dehydrogenase fragment of the NADH:ubiquinone oxidoreductase (complex I) from *Escherichia coli*, *Biochemistry 37*, 1861−1867.
27. Bungert, S., Krafft, B., Schlesinger, R., and Friedrich, T. (1999) One-step purification of the NADH dehydrogenase fragment of the *Escherichia coli* complex I by means of Strep-tag affinity chromatography, *FEBS Lett. 460*, 207−211.
28. Wallace, B. J., and Young, I. G. (1977) Role of quinones in electron transport to oxygen and nitrate in *Escherichia coli*. Studies with a ubiA- menA- double quinone mutant, *Biochim. Biophys. Acta 461*, 84−100.
29. Spehr, V., Schlitt, A., Scheide, D., Guenebaut, V., and Friedrich, T. (1999) Overexpression of the *Escherichia coli nuo*-operon and isolation of the overproduced NADH:ubiquinone oxidoreductase (complex I), *Biochemistry 38*, 16261−16267.
30. Hanahan, D. (1983) Studies on transformation of *Escherichia coli* with plasmids, *J. Mol. Biol. 166*, 557−580.
31. Studier, F. W., and Moffatt, B. A. (1986) Use of bacteriophage T7 RNA polymerase to direct selective high-level expression of cloned genes, *J. Mol. Biol. 189*, 113−130.
32. Datsenko, K. A., and Wanner, B. L. (2000) One-step inactivation of chromosomal genes in *Escherichia coli* K-12 using PCR products, *Proc. Natl. Acad. Sci. U.S.A. 97*, 6640−6645.
33. Birnboim, H. C., and Doly, J. (1979) A rapid alkaline extraction procedure for screening recombinant plasmid DNA, *Nucleic Acids Res. 7*, 1513−1523.
34. Leif, H., Sled, V. D., Ohnishi, T., Weiss, H., and Friedrich, T. (1995) Isolation and characterization of the proton-translocating NADH: ubiquinone oxidoreductase from *Escherichia coli*, *Eur. J. Biochem. 230*, 538−548.
35. Friedrich, T., van, H. P., Leif, H., Ohnishi, T., Forche, E., Kunze, B., Jansen, R., Trowitzsch-Kienast, W., Höfle, G., Reichenbach, H., and Weiss, H. (1994) Two binding sites of inhibitors in NADH: ubiquinone oxidoreductase (complex I). Relationship of one site with the ubiquinone-binding site of bacterial glucose: ubiquinone oxidoreductase, *Eur. J. Biochem. 219*, 691−698.
36. Flemming, D., Hellwig, P., and Friedrich, T. (2003) Involvement of tyrosines 114 and 139 of subunit NuoB in the proton pathway around cluster N2 in *Escherichia coli* NADH:ubiquinone oxidoreductase, *J. Biol. Chem. 278*, 3055−3062.
37. Schagger, H., and von Jagow, G. (1987) Tricine-sodium dodecyl sulfate-polyacrylamide gel electrophoresis for the separation of proteins in the range from 1 to 100 kDa, *Anal. Biochem. 166*, 368−379.
38. Waletko, A., Zwicker, K., Abdrakhmanova, A., Zickermann, V., Brandt, U., and Kerscher, S. (2005) Histidine 129 in the 75-kDa subunit of mitochondrial complex I from *Yarrowia lipolytica* is not a ligand for [Fe4S4] cluster N5 but is required for catalytic activity, *J. Biol. Chem. 280*, 5622−5625.
39. Hagen, W. R., Silva, P. J., Amorim, M. A., Hagedoorn, P. L., Wassink, H., Haaker, H., and Robb, F. T. (2000) Novel structure and redox chemistry of the prosthetic groups of the iron-sulfur flavoprotein sulfide dehydrogenase from *Pyrococcus furiosus*; evidence for a [2Fe-2S] cluster with Asp(Cys)3 ligands, *J. Biol. Inorg. Chem. 5*, 527−534.
40. Beinert, H. (2000) Iron-sulfur proteins: ancient structures, still full of surprises, *J. Biol. Inorg. Chem. 5*, 2−15.
41. Weidner, U., Geier, S., Ptock, A., Friedrich, T., Leif, H., and Weiss, H. (1993) The gene locus of the proton-translocating NADH: ubiquinone oxidoreductase in *Escherichia coli*. Organization of the 14 genes and relationship between the derived proteins and subunits of mitochondrial complex I, *J. Mol. Biol. 233*, 109−122.
42. Sled, V. D., Friedrich, T., Leif, H., Weiss, H., Meinhardt, S. W., Fukumori, Y., Calhoun, M. W., Gennis, R. B., and Ohnishi, T. (1993) Bacterial NADH-quinone oxidoreductases: iron-sulfur clusters and related problems, *J. Bioenerg. Biomembr. 25*, 347−356.
43. Yano, T., Sklar, J., Nakamaru-Ogiso, E., Takahashi, Y., Yagi, T., and Ohnishi, T. (2003) Characterization of cluster N5 as a fast-relaxing [4Fe-4S] cluster in the Nqo3 subunit of the proton-translocating NADH-ubiquinone oxidoreductase from *Paracoccus denitrificans*, *J. Biol. Chem. 278*, 15514−15522.
44. Finel, M. (1993) The proton-translocating NADH: ubiquinone oxidoreductase: a discussion of selected topics, *J. Bioenerg. Biomembr. 25*, 357−366.
45. Cross, M., Xiao, Z., Maes, E. M., Czernuszewicz, R. S., Drew, S. C., Pilbrow, J. R., George, G. N., and Wedd, A. G. (2002) Removal of a cysteine ligand from rubredoxin: assembly of Fe(2)S(2) and Fe(S-Cys)(3)(OH) centres. *J. Biol. Inorg. Chem. 7*, 781−790.
46. Furnham, N., Dore, A. S., Chirgadze, D. Y., de Bakker, P. I., Depristo, M. A., and Blundell, T. L. (2006) Knowledge-based real-space explorations for low-resolution structure determination, *Structure 14*, 1313−1320.
47. Emsley, P., and Cowtan, K. (2004) Coot: model-building tools for molecular graphics, *Acta Crystallogr., Sect. D: Biol. Crystallogr. 60*, 2126−2132.

BI700371C